Photodissociation of Propylene Sulfide at 193 nm: A Photofragment Translational Spectroscopy Study with VUV Synchrotron Radiation

Fei Qi†

Chemical Sciences Division, Ernest Orlando Lawrence Berkeley National Laboratory, Berkeley, California 94720

Arthur G. Suits*

Department of Chemistry, Stony Brook University, Stony Brook, New York 11794-3400, and Chemistry Department, Brookhaven National Laboratory, Upton, New York 11973

Received: May 7, 2002; In Final Form: August 14, 2002

Photodissociation of propylene sulfide at 193 nm has been studied using photofragment translational spectroscopy. Five primary dissociation channels were observed: $S(^1D) + C_3H_6$, $S(^3P) + C_3H_6$, $HS + C_3H_5$, $H_2S + C_3H_4$, and $CH_3 + C_2H_3S$. Tunable synchrotron radiation was used to selectively probe reaction products. The $S + C_3H_6$ channel was identified to be a dominant channel with a branching ratio of 2.6:1 for $S(^1D)$:$S(^3P)$. Multiple components in the time-of-flight spectra of $S(^1D)$ were observed. They are ascribed to dissociation from different potential energy surfaces. These results complement our previous study of ethylene sulfide photodissociation at 193 nm [Qi, F.; et al. *J. Chem. Phys.* **2000**, *112*, 10707. Qi, F.; et al. *J. Am. Chem. Soc.* **2001**, *123* (2), 148].

1. Introduction

Sulfur-containing hydrocarbons are important intermediates in combustion and atmospheric chemistry. These species may play a significant role in the atmospheric sulfur cycle and contribute to acid rain and atmospheric aerosols.[1−7] In addition to these practical aspects of the importance of these molecules, their photodissociation is an interesting topic both from fundamental theoretical and experimental perspectives. In general these are complex processes, so it is important to measure the dissociation products accurately and unambiguously to develop a full understanding of the dissociation mechanisms. We have studied 193 nm photodissociation of ethylene sulfide probed via tunable synchrotron radiation,[8] which was used as a universal but selective probe of the reaction products, to reveal new aspects of ethylene sulfide photodissociation. For example, our study showed that the $S(^1D) + C_2H_4(^1A_g)$ channel dissociates on three different potential energy surfaces. The $S + C_2H_4$ channel was found to be dominant, with a branching ratio of $S(^3P)$:$S(^1D) = 1.4$:1. Furthermore, our results also suggested possible formation of excited triplet ethylene $C_2H_4(^3B_{1u})$ via 193 nm photodissociation of ethylene sulfide.[9] Propylene sulfide (methylthiirane) is a derivative of ethylene sulfide (see Figure 1), and both show very similar photoabsorption spectra in the UV region, but with different relative intensities.[10] Although Clark and Simpson observed a strong absorption peak at 192.2 nm for both species, they did not give a detailed assignment.[10] Later, Tokue and co-workers reinvestigated the UV absorption spectrum of ethylene sulfide and thietane, and they assigned the peak at 192.2 nm in ethylene sulfide to 4p Rydberg series.[11] However, no detailed assignment for propylene sulfide was reported for the peaks beginning at 192.2 nm. On the basis of the similarity of both the structure and absorption spectrum (near 192.2 nm) for ethylene sulfide and propylene sulfide, the peak near 192.2 nm for propylene sulfide may also be a 4p Rydberg transition.

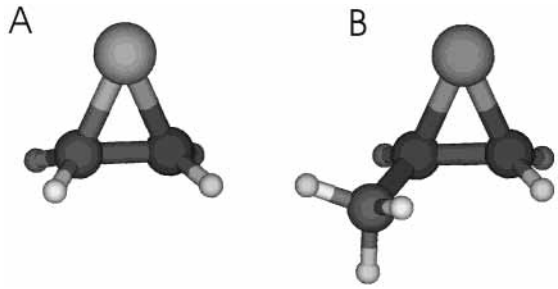

Figure 1. Ball-and-stick models of ethylene sulfide (A) and propylene sulfide (B).

Chin and co-workers investigated the thermal decomposition of propylene sulfide and ethylene sulfide in a flow system via monitoring photoelectron spectroscopy of the fragments.[12] Similar decomposition patterns were observed in both systems. S, C_3H_6, H_2S, and CS_2 were observed as major products with minor products of C_2H_2, C_2H_4, and $CH_3C{\equiv}CH$. Furthermore, they suggested that propylene sulfide converted into *cis*- and *trans*-prop-1-ene-1-thiol ($CH_3CH{=}CHSH$) as the first step of the ring-opening reaction at high temperature (>600 °C). However, these pyrolysis studies detected only the final products following multiple collisions and subsequent competition with secondary and tertiary chemical reactions.[12] Our study was performed under collision-free conditions in a supersonic molecular beam. Furthermore, vacuum ultraviolet (VUV) photoionization instead of electron impact ionization has many advantages for detecting dissociation products.[8,13,14]

* To whom correspondence should be addressed. E-mail: arthur.suits@sunysb.edu.

† Present address: Combustion Research Facility, Sandia National Laboratories, Livermore, CA 94550.

10.1021/jp026084a CCC: $22.00
Published on Web 10/22/2002

In this study, we have measured the time-of-flight (TOF) spectra of photofragments from the photolysis of propylene sulfide using photofragment translational spectroscopy (PTS) with probe by photoionization using tunable undulator radiation. Five primary dissociative channels have been identified, including three closed shell channels (1, 2, and 4) and two radical channels (3 and 5), as summarized by processes 1−5. All

$$C_3H_6S + h\nu_{193nm} \rightarrow S(^1D) + C_3H_6 \quad (1)$$

$$C_3H_6S + h\nu_{193nm} \rightarrow S(^3P) + C_3H_6 \quad (2)$$

$$C_3H_6S + h\nu_{193nm} \rightarrow HS + C_3H_5 \quad (3)$$

$$C_3H_6S + h\nu_{193nm} \rightarrow H_2S + C_3H_4 \quad (4)$$

$$C_3H_6S + h\nu_{193nm} \rightarrow CH_3 + C_2H_3 \quad (5)$$

observed channels are similar to photodissociation of ethylene sulfide at 193 nm, except we do not observe the H atom elimination channel in the case of propylene sulfide. The analysis and interpretation of these results is supported by the accompanying paper[15] describing the results of G3 calculations on this system.

2. Experimental Section

The experiments were performed on Chemical Dynamics Beamline 9.0.2.1 of the Advanced Light Source at Berkeley using a rotatable source molecular beam apparatus described in detail elsewhere.[16] Helium was bubbled through a room-temperature propylene sulfide sample (>98% purity purchased from Aldrich). The total pressure was about 800 Torr, yielding a mixture of ~5% propylene sulfide in He. The mixture was expanded through a pulsed valve with a 1 mm nozzle into the source chamber. The nozzle of the valve was heated to ~60 °C to avoid cluster formation. The resulting molecular beam was collimated with two skimmers, and the average molecular beam velocity and speed ratio were measured to be 1356 m/s and 11.0, respectively, accomplished via the hole-burning technique at the parent ion mass ($m/e = 74$). The beam parameters were determined by fitting laser-induced depletion profiles and assuming a number density distribution $f(v) \propto v^2 e^{-((v/\alpha)-S)^2}$.[17−19]

The molecular beam was intersected at 90° with an unpolarized ArF excimer (193 nm) laser beam. The laser beam was focused to a 2 × 4 mm^2 spot on the axis of rotation of the molecular beam source and aligned perpendicular to the plane containing the molecular beam and detector axes. Photofragments entering the triply differentially pumped detector region were photoionized using tunable synchrotron radiation. The flight length of neutral photofragments is 15.2 cm, that is, the distance between the photodissociation and the photoionization region. The undulator light source, described in detail elsewhere,[20] has a flux of 10^{16} photons/s (quasi-continuous), an energy bandwidth of about 2.2%, and a cross section in the probe region of 0.05 × 0.17 mm^2 (fwhm).[20] A gas filter filled with about 25 Torr Ar was used to eliminate higher harmonics of the undulator radiation.[21] A MgF_2 optical filter was also used to eliminate small contamination of the probe light by higher energy photons when the probing energy was below 11.0 eV. The photoionized products were mass selected by a quadrupole mass filter and the ions were counted with a Daly ion counter. Time-of-flight spectra of the neutral products were measured with a multichannel scaler (MCS) whose bin width (dwell time) was fixed at 1 or 2 μs for the measurements reported here. Timing sequences for the laser, pulsed valve, and the MCS were controlled using a digital delay generator. Laser power dependence was measured for all observed channels. Care was taken to ensure that the TOF data were free of multiphoton effects.

The tunability of the VUV light source allowed for the measurements of photoionization efficiency (PIE) spectra and for the selective ionization of products with very low background counts. A series of TOF spectra, recorded at a fixed angle for different photoionization energies, were normalized for the probe photon flux and integrated to obtain the PIE spectra.

3. Results

TOF spectra of photofragments from photodissociation of propylene sulfide at 193 nm have been measured from 10° to 40°. Signals at $m/e = 59$, 58, 42, 41, 40, 34, 33, and 32 were detected. These correspond to $C_2H_3S^+$, $C_2H_2S^+$, $C_3H_6^+$, $C_3H_5^+$, $C_3H_4^+$, H_2S^+, HS^+, and S^+, respectively. A forward convolution fit to the data was used to obtain center-of-mass translational energy distributions, $P(E_T)$.[22] A newly developed program, CMLAB3, was used to fit all the data.[23−25] In all the TOF spectra shown here, the open circles represent the experimental data, the dash lines and the dot lines are single channel contributions to the forward convolution fit, and the solid lines are the overall fit to the data.

3.1. S + C_3H_6 Channels. The ionization potentials (IPs) of the sulfur atom are well-known to be 10.36 and 9.21 eV for the ground state S(^{3}P) and the first excited state S(^{1}D), respectively.[26,27] Thus, in these studies the S(^{1}D) atom can be selectively ionized by using tunable VUV light at 9.5 eV, whereas contributions from both S(^{3}P) and S(^{1}D) appear at 10.8 eV. We used this method to selectively detect S(^{3}P) and S(^{1}D) from ethylene sulfide in a previous study.[8,28]

a. TOF Spectra of m/e 32 at 9.5 eV Photoionization Energy. Parts a and b of Figure 2 show TOF spectra of $m/e = 32$ with the indicated scattering angles and a probe photon energy of 9.5 eV. This corresponds to the first excited state S(^{1}D), because the photon energy used here is below the IP (10.36 eV) of the ground state sulfur S(^{3}P). A translational energy distribution $P(E_T)$, shown as the solid line in Figure 3a, was used to fit the TOF data very well. Thus, this $P(E_T)$ corresponds to process 1 (S(^{1}D) + C_3H_6). The $P(E_T)$ indeed includes three components, if we take a look in detail. In the case of ethylene sulfide, these three components were separated very clearly.[8] To explain their formation mechanism conveniently, and to compare with results of ethylene sulfide, we divided the $P(E_T)$ into three distributions, which are labeled as **A**, **B**, and **C**, shown in Figure 3a. These distributions are peaked roughly at 31, 15, and 3 kcal/mol, respectively. Each distribution is assigned to dissociation from different potential energy surfaces, as will be discussed later. An average translational energy for this channel was derived to be 24.1 kcal/mol with a maximum translational energy of 53 kcal/mol.

Depending on the structure of mass 42 (C_3H_6), two possible dissociation channels are allowed energetically. They are

$$C_3H_6S + h\nu_{193nm} \rightarrow S(^1D) + C_3H_6 \text{ (propylene)} \qquad \Delta H_{rxn} = -53.2 \text{ kcal/mol} \quad (1a)$$

$$C_3H_6S + h\nu_{193nm} \rightarrow S(^1D) + C_3H_6 \text{ (cyclopropane)} \qquad \Delta H_{rxn} = -45.2 \text{ kcal/mol} \quad (1b)$$

Here the heats of formation of propylene sulfide, propylene, cyclopropane, and S(^{1}D) are 2.74,[29] 4.78,[26] 12.79,[26] and 92.8[27] kcal/mol, respectively. In each case, the available energy is 53.2

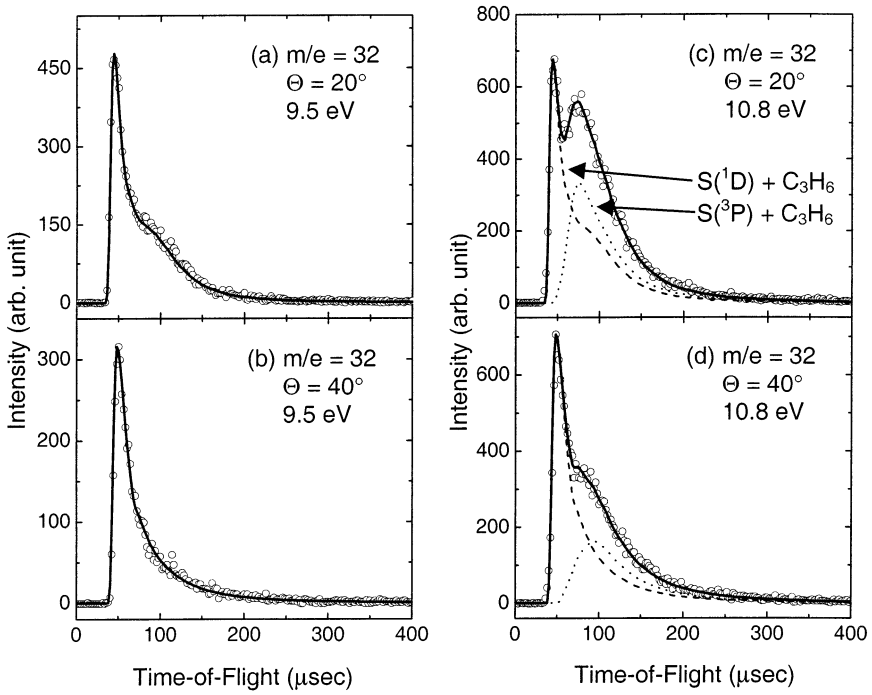

Figure 2. TOF spectra for *m/e* 32 (S): (a) 9.5 eV, 20°, and (b) 9.5 eV, 40° [(○) experimental data; (—) forward convolution fit using translational energy distribution $P(E_T)$ (—) of (a)]; (c) 10.8 eV, 20°, and (d) 10.8 eV, 40° [(○) experimental data; (---, ···) single channel contributions to the forward convolution fit using translational energy distributions $P(E_T)$ of (a) and of (b), respectively; (—) overall fit].

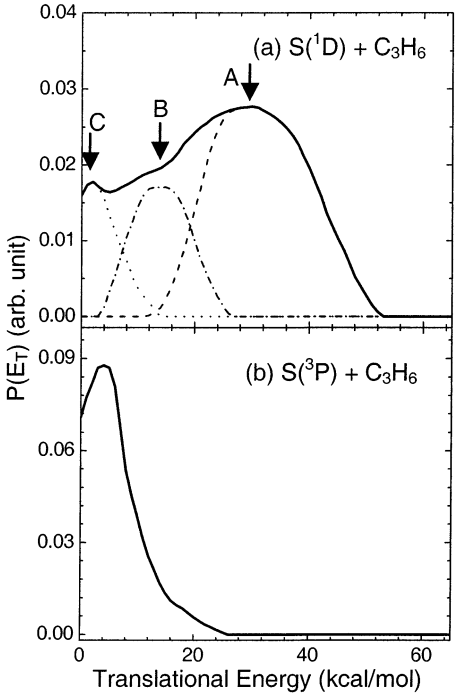

Figure 3. Translational energy distributions, $P(E_T)$'s, for the S + C_3H_6 channel: (a) S(^{1}D) + C_3H_6; (b) S(^{3}P) + C_3H_6.

kcal/mol for reaction 1a and 45.2 kcal/mol for reaction 1b, respectively. However, the observed maximum translational energy for this channel is 53 kcal/mol, which is beyond the available energy of the reaction 1b. Thus, a significant portion of the C_3H_6 must be assigned to propylene.

b. TOF Spectra of m/e 32 at 10.8 eV Photoionization Energy. The above measurements were repeated at 10.8 eV, and the TOF spectra are shown in Figure 2c,d. Two peaks are clearly observed in the TOF spectra at the scattering angle of 20°. At this probe energy, both excited state S(^{1}D) and ground state S(^{3}P) products contribute, but no S atom signal will arise from fragmentation of larger species (C_2H_3S, HS, and H_2S), because the probe energy is below the appearance energies of the S atom from these larger species (appearance energies for S^+ from these molecules range from 13.4 eV (H_2S) to 14.4 eV, on the basis of thermochemical cycles using NIST Webbook thermochemistry[30,31] or, for C_2H_3S, from the heat of formation given in ref 8). Although the internal energy could shift these appearance energies to lower values, it is unlikely that this effect will lead to shifts greater than 2 eV with significant yield. The $P(E_T)$ of Figure 3a fits the fast part of the TOF spectra. An additional translational energy distribution $P(E_T)$, shown in Figure 3b, was used to fit the slow peak. This $P(E_T)$ has an average translational energy of 6.5 kcal/mol. The $P(E_T)$ of Figure 3b actually corresponds to the channel S(^{3}P) + C_3H_6.

Considering the different isomers for mass 42 (C_3H_6), two possible dissociation channels are allowed energetically. They are

$$C_3H_6S + h\nu_{193nm} \rightarrow S(^3P) + C_3H_6 \text{ (propylene)} \qquad \Delta H_{rxn} = -79.7 \text{ kcal/mol} \quad (2a)$$

$$C_3H_6S + h\nu_{193nm} \rightarrow S(^3P) + C_3H_6 \text{ (cyclopropane)} \qquad \Delta H_rH_{xn} = -71.7 \text{ kcal/mol} \quad (2b)$$

Here the heat of formation of S(^{3}P) is 66.3 kcal/mol.[26] The maximum translational energy was derived to be 26 kcal/mol, still within the available energies of both reactions 2a and 2b. Merely considering the energy distribution, it is difficult to distinguish which structure is formed from photodissociation of propylene sulfide.

c. Branching Ratio for S(^{1}D) and S(^{3}P). Branching ratio measurements obtained using photoionization near the ionization threshold would be misleading because the ionization cross section, σ_i, for S(^{1}D) and S(^{3}P) can be different near their respective onsets and are often perturbed by strong autoionization resonances.[32−34] Previous measurements have shown the photoionization cross sections σ_i to be similar for the two states

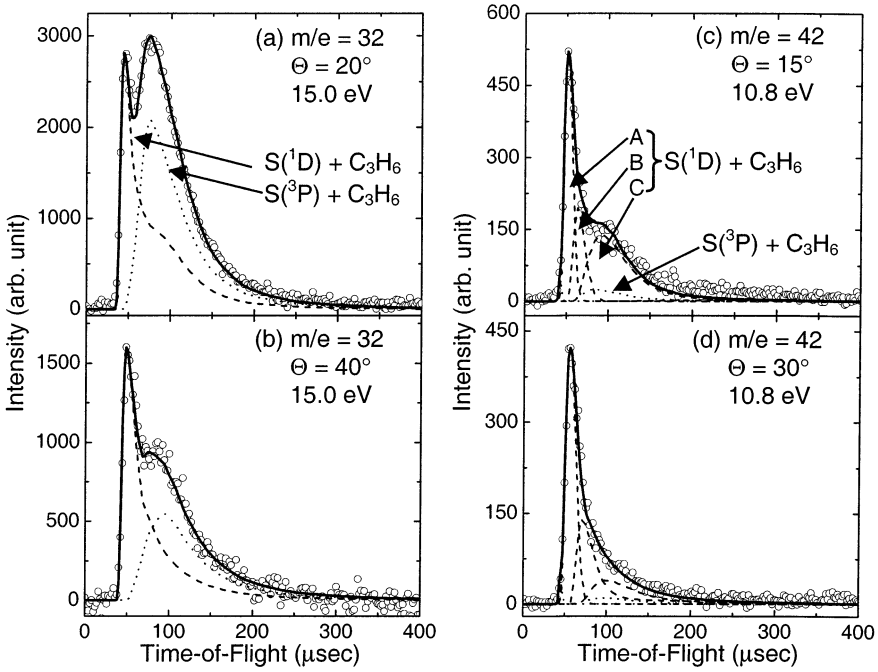

Figure 4. TOF spectra for *m*/*e* 32 (S) and 42 (C_3H_6): (a) *m*/*e* = 32, 20°, 15.0 eV, and (b) *m*/*e* = 32, 40°, 15.0 eV [(○) experimental data; (---, ···) single channel contributions to the forward convolution fit using translational energy distributions $P(E_T)$ of Figure 2a,b, respectively; (—) overall fit]; (c) *m*/*e* = 42, 15°, 10.8 eV, and (d) *m*/*e* = 42, 30°, 10.8 eV [(○) experimental data; (---) single channel contribution to the forward convolution fits using $P(E_T)$'s (labeled as **A**, **B**, and **C**) in Figure 2a; (···) single channel contributions using the translational energy distribution of Figure 2b; (—) overall fit].

at the probe energy of 15.0 eV.[8,28] Thus, measurements of TOF spectra of *m*/*e* 32 were made at 15.0 eV photoionization energy and are shown in Figure 4a,b, and were fitted using the two $P(E_T)$'s of Figure 3. According to this fit, the branching ratio of $S(^1D):S(^3P)$ is 0.72:0.28.

d. TOF Spectra of m/e 42. Parts c and d of Figure 4 show the TOF spectra of *m*/*e* 42, the momentum-matched partner of *m*/*e* 32, at the indicated scattering angles and 10.8 eV photon energy. The TOF spectra of *m*/*e* 42 were fitted using the $P(E_T)$'s shown in Figure 3, with some substantial adjustment of their relative contributions. The identity of the mass 42 product is difficult to establish with certainty. The IPs of the two possible isomers, propylene and cyclopropane, are 9.73 and 9.86 eV, respectively,[26] too close to be discriminated on the basis of ionization onset, given the substantial internal energy in these products. On the basis of the difference in energetics, and the anticipated dynamics outlined in the discussion below, we suspect that the propylene product will be dominant. The momentum-matching between mass 42 and 32 is far from satisfactory. In fact, the slow contribution to the mass 42 signal, which formed in conjunction with $S(^3P)$, is significantly suppressed. The ratios of the different contributions of the mass 32 fits used in fitting the mass 42 data were 0.70 ($S(^1D)-A$), 0.191 ($S(^1D)-B$), 0.088 ($S(^1D)-C$), and 0.021 ($S(^3P)$), respectively. Overall, these were scaled arbitrarily (allowing for different ionization cross sections for different internal energy distributions, for example), but these same ratios were used in fitting all angles. Given that, for formation of propylene, for example, this product will have roughly 3 eV internal energy, we anticipate possible fragmentation upon ionization, even for "soft" photoionization near threshold. Indeed, examination of the mass 41 and 40 signal shows that the slow contribution from the mass 42 primary process may well appear at these lower masses; the distributions are too similar to identify this as a distinct contribution. In addition to possible dissociative ionization of hot products, there is also the possibility of H_2 loss from the excited C_3H_6 leading to selective depletion of slow mass 42. In all these cases, we feel the smaller S-containing fragments give the primary distributions reliably, and these have then been used as the principal basis in all the fits to the hydrocarbon fragments at lower masses, as seen below.

3.2. HS + C_3H_5 Channel. TOF spectra of *m*/*e* 33 and 41 were measured. This corresponds to the HS radical loss channel as follows:

$$C_3H_6S + h\nu_{193nm} \rightarrow HS + C_3H_5 \qquad \Delta H_{rxn} = -75.7 \text{ kcal/mol} \quad (3)$$

Here the heats of formation of HS and C_3H_5 (allyl radical) are 34.12[26] and 40.9 kcal/mol,[35] respectively. This HS radical elimination channel was observed in the 193 nm photodissociation of ethylene sulfide. Parts a and b of Figure 5 show the TOF spectra of *m*/*e* 33 (HS) at the indicated scattering angles and 11.5 eV probe energy. The data were fitted using the translational energy distribution $P(E_T)$ shown in Figure 6a. This translational energy distribution has an average energy of 8.6 kcal/mol with a peak at 4 kcal/mol. The energy distribution extends to about 48 kcal/mol.

The momentum-matched fragment (mass 41) of *m*/*e* 33 was also measured; the data are shown in Figure 5c,d at the probe photon energy of 11.0 eV and the scattering angles of 15° and 30°, respectively. Two components were clearly discerned. The $P(E_T)$ of Figure 6a just fits the slow part. The fast peak was fitted by using the $P(E_T)$'s of Figure 3. In this case, the $P(E_T)$'s of Figure 3 were combined to one $P(E_T)$ according to their relative contributions to fit the 15 eV TOF spectra of mass 32. Hence, the fast peak comes from the dissociative ionization of the larger fragment C_3H_6 as discussed above. The appearance energy of $C_3H_5^+$ from propylene is 11.86 eV.[31] However, the C_3H_6 has substantial internal energies that may shift this appearance energy lower, even for the faster product formed in

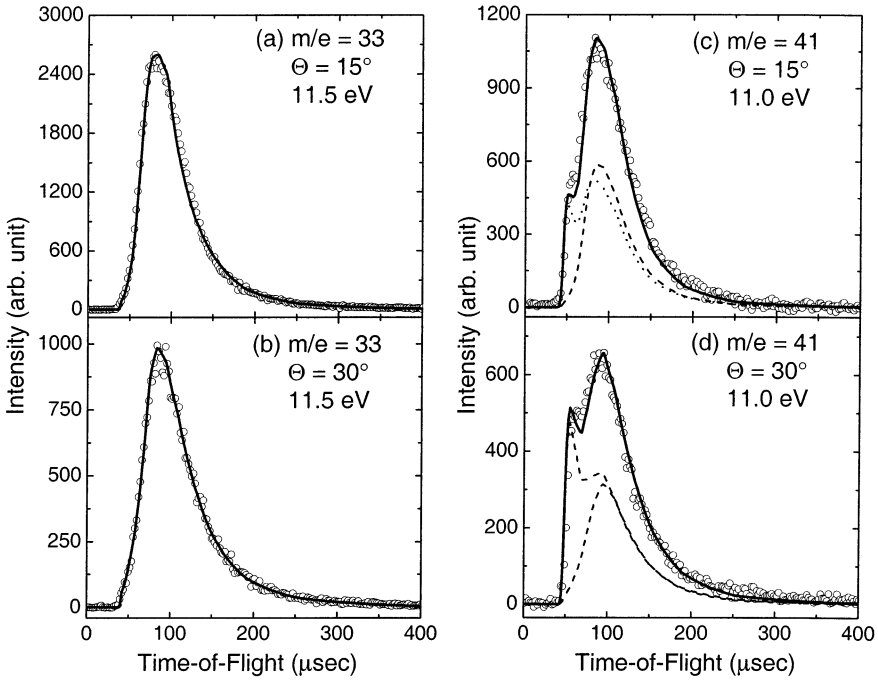

Figure 5. TOF spectra for *m*/*e* 33 (HS) and 41 (C_3H_5) with the indicated photoionization energies and scattering angles. The open circles are the experimental data. For (a) and (b), the data were fit using the translational energy distribution of (a). For (c) and (d), the dashed line is single channel contribution to the forward convolution fit using $P(E_T)$ of (a), the dotted line is the single channel contribution using a $P(E_T)$ by combining all $P(E_T)$'s of Figure 2.

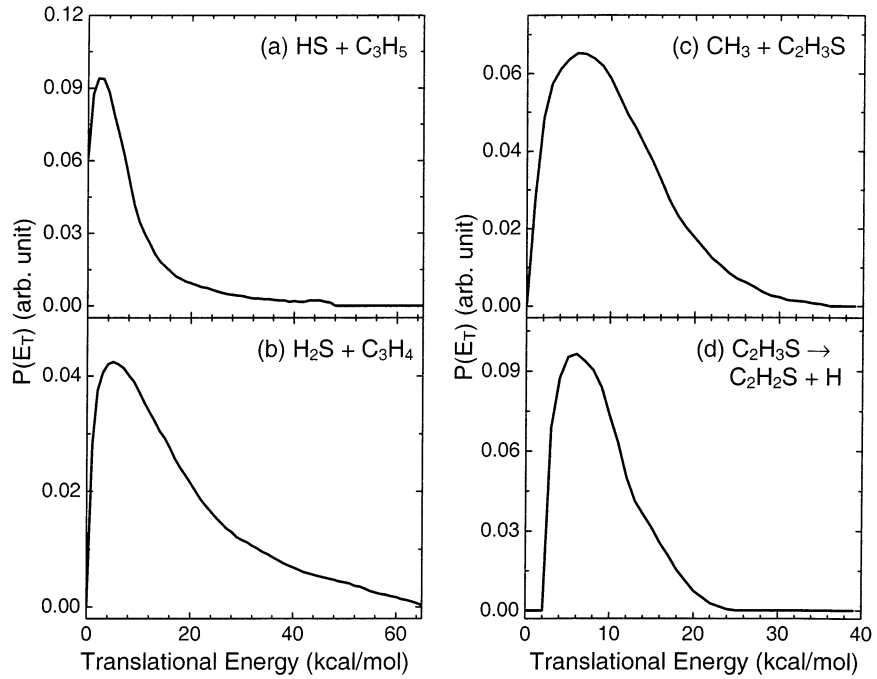

Figure 6. Translational energy distributions with indicated dissociation channels: (a) HS + C_3H_5; (b) H_2S + C_3H_4; (c) CH_3 + C_2H_3S; (d) secondary dissociation of $C_2H_3S \rightarrow C_2H_2S$ + H.

conjunction with S(^{1}D), so that dissociation ionization from C_3H_6 could occur at 11.0 eV.

3.3. H_2S + C_3H_4 Channel. Parts a and b of Figure 7 show the TOF spectra of *m*/*e* 34 (H_2S) at 11.5 eV photon energy and the scattering angles of 15° and 30°, respectively. A translational energy distribution $P(E_T)$, shown in Figure 6b, was used to fit the data. The TOF spectra of *m*/*e* 40 (C_3H_4), the momentum-matched fragment of *m*/*e* 34 (H_2S), are shown in Figure 7c,d with the 10.8 eV photon energy and a scattering angle of 15° and 30°, respectively. Two translational energy distributions were used to fit the data: $P(E_T)$ of Figure 6b fits the fast part with a small contribution (the dashed line); $P(E_T)$ of Figure 6a fits the slow part with a large contribution (the dotted line). Hence, most of the C_3H_4 signal arises from the dissociative ionization of the radical C_3H_5 or the primary propylene product at photoionization energy of 10.8 eV.

The TOF data of *m*/*e* 34 and 40 corresponds to the H_2S + C_3H_4 channel. An average translational energy distribution was determined to be 17.6 kcal/mol, with a maximum energy of about 67 kcal/mol. An exit barrier of roughly 6 kcal/mol was estimated for this channel. Similar to C_3H_6, C_3H_4 also has some different isomers: allene, propyne, and cyclopropene. The

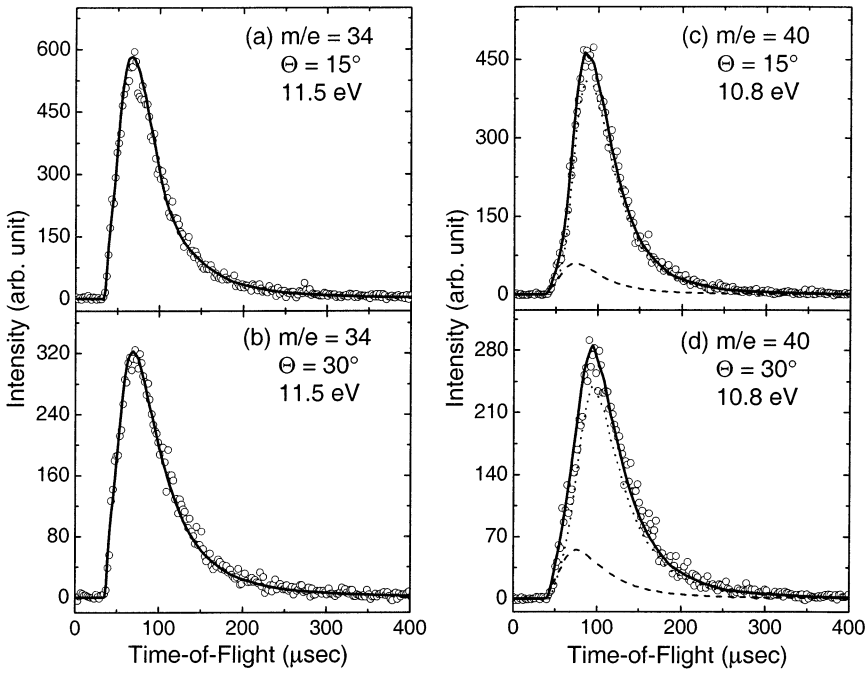

Figure 7. TOF spectra for *m*/*e* 34 (H_2S) and 40 (C_3H_4) with the indicated photoionization energies and scattering angles. The open circles are the experimental data. For (a) and (b), the data were fit using the translational energy distribution $P(E_T)$ shown in Figure 5b. For (c) and (d), the dashed and dotted lines are the single channel contributions to the forward convolution fit using $P(E_T)$'s of Figure 5b,a, respectively. The solid line is the overall fit.

dissociation including three energetically allowed structures are listed as follows:

$$C_3H_6S + h\nu_{193nm} \rightarrow H_2S + C_3H_4 \text{ (allene)} \qquad \Delta H_{rxn} = -110.1 \text{ kcal/mol} \quad (4a)$$

$$C_3H_6S + h\nu_{193nm} \rightarrow H_2S + C_3H_4 \text{ (propyne)} \qquad \Delta H_{rxn} = -111.5 \text{ kcal/mol} \quad (4b)$$

$$C_3H_6S + h\nu_{193nm} \rightarrow H_2S + C_3H_4 \text{ (cyclopropene)} \qquad \Delta H_{rxn} = -89.4 \text{ kcal/mol} \quad (4c)$$

Here the heats of formation of H_2S, allene, propyne, and cyclopropene are −4.93, +45.55, +44.21, and +66.26 kcal/mol, respectively.[26]

It is hard to assign mass 40 to any particular isomer just on the basis of the thermochemical information, because the heats of formation for propyne and allene are just 1.34 kcal/mol apart. Their ionization potentials are different, however: the IP of propyne is 10.36 eV, and the IP of allene is 9.69 eV.[26] Tunable synchrotron radiation may sometimes be able to selectively probe the product; however, in this case the *m*/*e* = 40 signal is dominated by fragmentation of hot products in the ionization step, so the photoionization spectra can provide little insight. Recent theoretical studies by Li and co-workers[42] at the G3 level of theory find a much lower barrier (76 vs 112 kcal/mol) for propyne formation than for allene formation from propylene sulfide, and this process likely exhibits a larger *A* factor as well. We thus assign the *m*/*e* = 40 product to propyne.

3.4. CH_3 Loss Channel. The CH_3 radical elimination channel as follows is the weakest of all observed channels:

$$C_3H_6S + h\nu_{193nm} \rightarrow CH_3 + C_2H_3S \qquad \Delta H_{rxn} = -43.5 \text{ kcal/mol} \quad (5)$$

Here the heats of formation of CH_3 and C_2H_3S are 34.84[26] and 72.1 kcal/mol,[8] respectively. Figure 8a shows TOF spectra of *m*/*e* 59 (C_2H_3S) at 10.5 eV photon energy and 15° scattering angle. The data were fit using a translational energy distribution shown in Figure 6c. This $P(E_T)$ fits the fast part of the TOF spectra (Figure 8b) of *m*/*e* 15 (CH_3), the momentum-matched fragment of mass 59. The maximum energy extends to 37 kcal/mol with an average translational energy of 10.3 kcal/mol.

A PIE curve of mass 59 was measured at a scattering angle of 15°, which is shown in Figure 9. The onset is about 8.7 eV. Li and co-workers performed a theoretical calculation on structures, energetics, and reactions of C_2H_3S radicals and $C_2H_3S^+$ ions.[36] They suggested that the thioformylmethyl radical is the most stable of all possible C_2H_3S isomers. The ionization potential of the thioformylmethyl radical was found to be 9.08 eV in their calculations.[36] It is not surprising that our value is 0.38 eV lower than theoretical result, because the C_2H_3S fragment has some internal energy.

The bond strength of C_2H_2S-H is estimated to be 28 kcal/mol from the heats of formation ($\Delta H°_{f0}$) of C_2H_3S (72.1 kcal/mol),[8] C_2H_2S (48.0 kcal/mol),[8] and H (52.01 kcal/mol).[26] Thus, the C_2H_3S radical has enough internal energy to undergo secondary dissociation (reaction 6):

$$C_2H_3S \rightarrow C_2H_2S + H \qquad \Delta H_{rxn} = 27.91 \text{ kcal/mol} \quad (6)$$

In fact, we did observe the signal of *m*/*e* 58 (C_2H_2S). The TOF spectra of *m*/*e* 58 at 10.8 eV photon energy and the 15° scattering angle is shown in Figure 8c, which was fit using the translational energy distribution of Figure 6d. If the C_2H_2S fragment is a primary channel, we should observe its stable momentum-matched fragment, mass 16 (CH_4). However, no signal was observed at *m*/*e* 16. Also, an attempt was made to detect the H atom loss channel by monitoring signal of *m*/*e* 73 at angles as close as 5° from the molecular beam. No signal was found, implying no evidence for H atom elimination at total translational energies above 5.8 kcal/mol; the corresponding

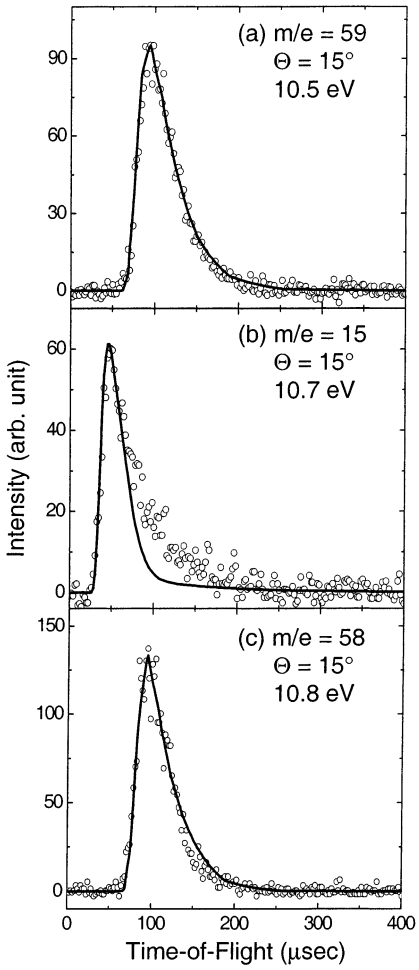

Figure 8. (a) TOF spectra for *m*/*e* 59 (C_2H_3S) at a scattering angle of 15° and photoionization energy of 10.5 eV. The open circles are the experimental data, and the solid lines are the forward convolution fits using the $P(E_T)$ in Figure 5c. (b) TOF spectra for *m*/*e* 15 (CH_3) at a scattering angle of 15° and photoionization energy of 10.7 eV. The open circles are the experimental data, and the solid lines are the forward convolution fits using the $P(E_T)$ in Figure 5c. (c) TOF spectra of *m*/*e* 58 (C_2H_2S) at 15° scattering angle and 10.8 eV photon energy. The data were fit using a translational energy distribution of Figure 5d.

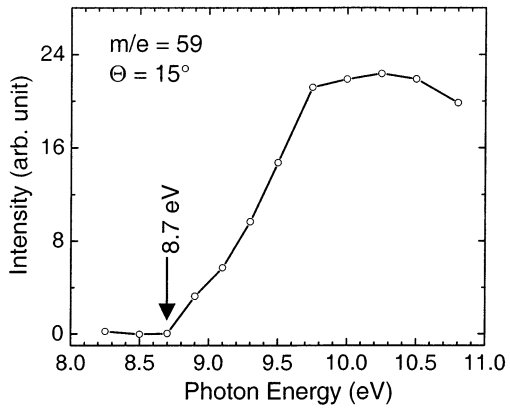

Figure 9. Photoionization efficiency curve of the C_2H_3S fragment measured at a scattering angle of 15°.

channel was observed in ethylene sulfide with an average translational energy release of 19 kcal/mol.

4. Discussion

Table 1 lists energy partitioning of all primary dissociation channels including total available energy (E_{avai}), maximum translational energy ($E_{max-trans}$), average translational energy ($\langle E_{trans}\rangle$), average internal energy ($\langle E_{int}\rangle$), and their ratios.

TABLE 1: Energy Partition of Different Dissociation Channels of Propylene Sulfide at 193 nm Excitation (kcal/mol)

dissociation channel	total available energy E_{avai}	maximum E_{trans}	averaged $\langle E_{trans}\rangle$	averaged $\langle E_{int}\rangle$	$\langle E_{trans}\rangle$/ $\langle E_{int}\rangle$
1	53.2	53	24.1	29.1	45.3/54.7
2	79.7	26	6.5	73.2	8.1/91.9
3	76.5	48	8.64	67.9	11.3/88.7
4	110.1	67	17.6	92.5	16.0/84.0
5	43.5	37	10.33	33.2	23.7/76.3

4.1. S + C_3H_6 Channels. Three components in the $P(E_T)$ of Figure 3a correspond to channels forming $S(^1D) + C_3H_6$. It is quite reminiscent of the analogous channels of $S(^1D) + C_2H_4$ from ethylene sulfide photodissociation at 193 nm, in which the three components were more clearly resolved. Because we see a similar trimodal translational energy distribution, and a similar absorption spectrum of propylene sulfide and ethylene sulfide,[10] we suspect their dissociation mechanisms may be of a similar nature, at least for this channel. In the following discussion, we use the C_{2v} labels to preserve the analogy to ethylene sulfide. It is assumed that propylene sulfide is excited to the second singlet excited state S_2 and then undergoes three different processes on singlet potential energy surfaces (PES): first, direct dissociation on the S_2 PES forms the fast $S(^1D)$ atoms; second, a coupling between S_2 and S_1 states gives the middle $S(^1D)$ fragment; third, the slow $S(^1D)$ comes from internal conversion on the ground state S_0.

The spin-forbidden channel, $S(^3P) + C_3H_6$, was also observed in this study. It is common to observe the spin-forbidden channel from the photodissociation of sulfur compounds: it has been seen in CS_2,[37] SO_2,[38] thiophene,[39,40] and ethylene sulfide.[8] The ring-opening reaction may be the first step to form a biradical (i.e., SCH_2CHCH_3) as Chin and co-workers suggested, which then undergoes intersystem crossing and internal conversion on the ground state. Furthermore, the translational energy distribution shows that most the available energy of this channel is kept as the internal energy of products, and less is transferred to the translational energy (see Table 1). A similar channel was observed in photodissociation of ethylene sulfide; however, the $S(^3P) + C_2H_4$ channel dissociates via two different methods: one is from the coupling between the excited state $^1A_1$ and the excited triplet state $^3B_2$ by the intersystem crossing, and another from internal conversion followed by intersystem crossing from the ground state.[8] The detailed mechanism could be deduced from theoretical calculations.

The branching ratio of $S(^1D):S(^3P)$ was measured at 193 nm excitation to be 0.72:0.28 for propylene sulfide, and 0.41:0.59 for ethylene sulfide,[8] respectively. The difference in the branching ratio could be caused by the disappearance of one channel ($S(^3P) + C_3H_6$ from the coupling of $^1A_1$ and $^3B_2$ states) mentioned above, or/and different ring strain for both systems.

Excited states of propylene have been studied by different groups.[41−43] The first triplet excited state $1^3A'(\pi\pi^*)$ is about 4.3 eV (99 kcal/mol) above the ground state propene ($\tilde{X}\ ^1A'$) for a vertical transition.[41] The available energies for reaction **1** and **2** are 53.2 and 79.7 kcal/mol, respectively. On the other hand, the first singlet excited state $1^1A''$ (π 3s) is 6.55 eV (151 kcal/mol) above the ground state.[41] However, the excited states of propylene cited here are for a vertical transition. In fact, the geometry of any possible excited propylene product could be distorted. The energy of the adiabatic transition to the triplet state should thus be lower, perhaps to the same extent (58 kcal/

mol) as in ethylene. A G3 theoretical calculation (reported in the following paper) suggests that the adiabatic singlet−triplet separation for propylene is 64 kcal/mol at 0 K.[15] This would place the available energy for the triplet propylene channel at about 16 kcal/mol. We see no corresponding peak in the translational energy distributions nor in the TOF spectra. This could be a consequence of several factors: (1) triplet propylene is produced, in analogy to the triplet ethylene inferred in ethylene sulfide dissociation, but its energy is higher, relatively, than ethylene, so that the peak is concealed under the dominant low energy product assigned to spin-forbidden dissociation via the ground state, or (2) no triplet propylene is produced in the case of propylene sulfide dissociation. The latter could arise from either energetic or dynamic considerations. To the best of our knowledge, no experimental report has appeared on the triplet excitation energy of propylene. A reliable value for this quantity would be helpful in sorting out these questions.

4.2. Other Dissociation Channels. All other dissociation channels likely undergo the ring-opening reaction forming the diradical, which can then undergo hydrogen migration to form *cis*- and *trans*-prop-1-ene-1-thiol ($CH_3CH{=}CH{-}SH$) or prop-1-ene-2-thiol ($CH_3C(SH){=}CH_2$) or other isomers, e.g., thioacetone ($(CH_3)_2C{=}S$) or allyl mercaptan ($CH_2{=}CH{-}CH_2{-}SH$). Both for mass 41 (C_3H_5) and mass 40 (C_3H_4) formation, it seems plausible that interaction of the S atom with the methyl hydrogens via cyclic transition states will be most important owing to geometric and energetic considerations, but this clearly requires more theoretical work to establish with any certainty. In general, products from excited state dissociation carry more translational energy and less internal energy than corresponding ground state dissociation processes. Comparing $\langle E_{trans}\rangle/\langle E_{int}\rangle$ of different channels in Table 1, unimolecular dissociation on the ground state by internal conversion is likely for reactions 2−5. In fact, the dissociation process is very complicated. More detailed theoretical investigations are desirable to interpret all of our observations.

5. Conclusion

This paper presents a photodissociation study of propylene sulfide at 193 nm excitation. Five primary dissociation channels were observed: $S(^1D) + C_3H_6$, $S(^3P) + C_3H_6$, $HS + C_3H_5$, $H_2S + C_3H_4$, and $CH_3 + C_2H_3S$. Tunable synchrotron radiation was used to selectively probe the reaction products. The $S + C_3H_6$ channel was identified to be a dominant channel with a branching ratio of 2.61:1 for $S(^1D):S(^3P)$. Multiple components in TOF spectra of $S(^1D)$ were clearly observed, and are ascribed to dissociation from different potential energy surfaces. In this measure, the results show striking similarities to our previous results for ethylene sulfide photodissociation, with the significant difference being the absence of a peak in the propylene sulfide analogous to that assigned to the production of triplet ethylene from ethylene sulfide.

Acknowledgment. We thank Dr. Osman Sorkhabi for his help. This work was supported by the Director, Office of Science, Office of Basic Energy Sciences, Chemical Sciences Division of the U.S. Department of Energy under contract No. DE-AC03-76SF00098 (LBNL) and DE-AC02-98CH1086 (BNL). The Advanced Light Source is supported by the Director, Office of Science, Office of Basic Energy Sciences, Materials Sciences Division of the U.S. Department of Energy, under the former contract.

References and Notes

(1) Farquhar, J.; Bao, H.; Thiemens, M. *Science* **2000**, *289*, 756.
(2) Farquhar, J.; Savarino, J.; Jackson, T. L.; Thiemens, M. H. *Nature* **2000**, *404*, 50.
(3) Kulmala, M.; Pirjola, L.; Makela, J. M. *Nature* **2000**, *404*, 66.
(4) Calvert, J. G.; Pitts, J. N. *Photochemistry*; Wiley: New York, 1996.
(5) Wayne, R. P. *Chemistry of Atmospheres*; Clarendon: Oxford, U.K., 1991.
(6) Yin, F.; Grosjean, D.; Seinfeld, J. H. *J. Geophys. Res.* **1986**, *91*, 14417.
(7) Andreae, M. O.; Raemdonck, H. *Science* **1983**, *221*, 744.
(8) Qi, F.; Sorkhabi, O.; Suits, A. G.; Chien, S.-H.; Li, W.-K. *J. Am. Chem. Soc.* **2001**, *123*, 148.
(9) Qi, F.; Sorkhabi, O.; Suits, A. G. *J. Chem. Phys.* **2000**, *112*, 10707.
(10) Clark, L. B.; Simpson, W. T. *J. Chem. Phys.* **1965**, *43*, 3666.
(11) Tokue, I.; Hiraya, A.; Shobatake, K. *J. Chem. Phys.* **1989**, *91*, 2808.
(12) Chin, W. S.; Chup, B. W.; Mok, C. Y.; Huang, H. H. *J. Chem. Soc., Perkin Trans.* **1994**, *2*, 883.
(13) Yang, X.; Blank, D. A.; Lin, J.; Heimann, P. A.; Wodtke, A. M.; Lee, Y. T.; Suits, A. G. Chemical Reaction Dynamics Using The Advanced Light Source. In *Synchrotorn Radiation Techniques in Industrial, and Materials Science*; D'Amico, K. L., Terminello, L. J., Shuh, D. K., Eds.; Plenum Press: New YorK, 1996; p 119.
(14) Blank, D. A. Molecular Beam Studies of Unimolecular and Bimolecular Chemical Reaction Dynamics Using VUV Synchrotorn Radiation as a Product Probe. Ph.D. Thesis, University of California, Berkeley, 1997.
(15) Lau, J. K.; Li, W. K.; Qi, F.; Suits, A. G. *J. Phys. Chem. A* **2002**, *106*, 11025.
(16) Yang, X.; Lin, J.; Lee, Y. T.; Blank, D. A.; Suits, A. G.; Wodtke, A. M. *Rev. Sci. Instrum.* **1997**, *68*, 3317−3326.
(17) Minton, T. K.; Felder, P.; Brudzynski, R. J.; Lee, Y. T. *J. Chem. Phys.* **1984**, *81*, 1759.
(18) Tzeng, W. B.; Yin, H. M.; Leung, W. Y.; Luo, J. Y.; Nourbakhsh, S.; Felsch, G. D.; Ng, C. Y. *J. Chem. Phys.* **1988**, *88*, 1658.
(19) Haas, B.-M.; Minton, T. K.; Felder, P.; Huber, J. R. *J. Phys. Chem.* **1991**, *95*, 5149.
(20) Heimann, P. A.; Koike, M.; Hsu, C. W.; Blank, D.; Yang, X. M.; Suits, A. G.; Lee, Y. T.; Evans, M.; Ng, C. Y.; Flaim, C.; Padmore, H. A. *Rev. Sci. Instrum.* **1997**, *68*, 1945−1951.
(21) Suits, A. G.; Heimann, P.; Yang, X. M.; Evans, M.; Hsu, C. W.; Lu, K. T.; Lee, Y. T.; Kung, A. H. *Rev. Sci. Instrum.* **1995**, *66*, 4841−4844.
(22) Zhao, X. Ph.D. Thesis, University of California at Berkeley, 1988.
(23) Harich, S. Ph.D., University of California at Santa Barbara, 1999.
(24) Harich, S.; Lin, J. J.; Lee, Y. T.; Yang, X. *J. Chem. Phys.* **1999**, *111*, 5.
(25) Wu, S. M.; Lin, J. J.; Lee, Y. T.; Yang, X. *J. Phys. Chem. A* **2000**, *104*, 7189.
(26) Lide, D. R. *Handbook of Chemistry and Physics*, 75th ed.; CRC: Boca Raton, FL, 1995−1996.
(27) *Atomic Energy Levels*; Moore, C. E., Ed.; National Bureau of Standards: Washington, DC, 1952; Vol. I.
(28) McGivern, W. S.; Sorkhabi, O.; Rizvi, A. H.; Suits, A. G.; North, S. W. *J. Chem. Phys.* **2000**, *112*, 5301.
(29) Sunner, S. *Acta Chem. Scand.* **1963**, *17*, 728.
(30) Afeefy, H. Y.; Liebman, J. F.; Stein, S. E. Neutral Thermochemical Data. In *NIST Chemistry Webbook, NIST Standard Reference Database Number 69*; Linstrom, P. J., Mallard, W. G., Eds.; NIST: Gaithersburg, MD, 2001.
(31) Lias, S. G.; Liebman, J. F. Ion Energetics Data. In *NIST Chemistry Webbook, NIST Standard Reference Database Number 69*; Linstrom, P. J., Mallard, W. G., Eds.; NIST: Gaithersburg, MD, 2001.
(32) Gibson, S. T.; Greene, J. P.; Ruscic, B.; Berkowitz, J. *J. Phys. B: At. Mol. Phys.* **1986**, *19*, 2825.
(33) Pratt, S. T. *Phys. Rev. A* **1988**, *38*, 1270.
(34) Chen, C. T.; Robicheaux, F. *Phys. Rev. A* **1994**, *50*, 3968.
(35) Tsang, W. *Heats of Formation of Organic Free Radicals by Kinetic Methods*; Blackie Academic and Professional: London, 1996.
(36) Chiu, S.-W.; Lau, K.-C.; Li, W.-K. *J. Phys. Chem. A* **2000**, *104*, 3028.
(37) Waller, I. M.; Hepburn, J. W. *J. Chem. Phys.* **1987**, *87*, 3261−8.
(38) Effenhauser, C. S.; Felder, P.; Huber, J. R. *Chem. Phys.* **1990**, *142*, 311−20.
(39) Hsu, C. W.; Liao, C. L.; Ma, Z. X.; Ng, C. Y. *J. Phys. Chem.* **1995**, *99*, 1760−1767.
(40) Qi, F.; Sorkhabi, O.; Rizvi, A. H.; Suits, A. G. *J. Phys. Chem. A* **1999**, *103*, 8351.
(41) Walker, I. C.; Abuain, T. M.; Palmer, M. H.; Beveridge, A. J. *Chem. Phys.* **1986**, *109*, 269.
(42) Bowman, C. R.; Miller, W. D. *J. Chem. Phys.* **1965**, *42*, 681.
(43) Derai, R.; Danon, J. *Chem. Phys. Lett.* **1977**, *45*, 134.